

Investigation of the correlation between diffuse infrared and ultrasound for transcranial ultrasound

This content has been downloaded from IOPscience. Please scroll down to see the full text.

2016 Biomed. Phys. Eng. Express 2 035016

(<http://iopscience.iop.org/2057-1976/2/3/035016>)

View [the table of contents for this issue](#), or go to the [journal homepage](#) for more

Download details:

IP Address: 139.137.128.60

This content was downloaded on 09/06/2016 at 23:24

Please note that [terms and conditions apply](#).

Biomedical Physics & Engineering Express



PAPER

Investigation of the correlation between diffuse infrared and ultrasound for transcranial ultrasound

Qi Wang, Mark Howell, Shota Shimizu, Sheronica James, Aref Smiley and Gregory T Clement

Department of Biomedical Engineering, Cleveland Clinic Lerner Research Institute, Cleveland, OH, USA

E-mail: wangq4@ccf.org

Keywords: transcranial ultrasound, human skull, diffuse infrared

RECEIVED
24 February 2016

REVISED
22 April 2016

ACCEPTED FOR PUBLICATION
13 May 2016

PUBLISHED
8 June 2016

Abstract

Over the past two decades the feasibility for using transcranial ultrasound as both a therapeutic and diagnostic tool has been established. Various aberration-correction techniques have been proposed to achieve transcranial focusing, including computed tomography-derived model based corrections, ultrasound-derived model based corrections, magnetic resonance acoustic radiation force techniques, and techniques involving the invasive introduction of an acoustic source or receiver into the brain. Here, we investigate the correlation between transcranial infrared light (IR) and transcranial ultrasound, where we examine whether IR could be an indicator of any of the key acoustic properties that affect transcranial transmission (signal attenuation, speed of sound, and bone density). Nine human skull samples were utilized in the study. The interior of each sample was illuminated over its inner surface using a diffuse light source. Light transmitted to the outer surface was detected by a 3 mm diameter 940 nm infrared sensor. Acoustic measurements were likewise obtained in a water tank using a 12.7 mm diameter 1 MHz source and a needle hydrophone receiver. Results reveal a positive correlation between the acoustic time-of-flight and optical intensity (the correlation coefficient is between 0.5 and 0.9). Subsequent investigation shows this correlation to hold independent of the presence or absence of dura mater on the samples. Poor correlation is observed between acoustic amplitude and optical intensity (the correlation coefficient is between 0.1 and 0.7).

1. Introduction

Although it has been reported that ultrasound can propagate through human skulls, including thicker parts of the bone [1, 2], coherent focusing generally requires some form of correction to offset wave distortion [3]. A variety of approaches for performing this offset have been proposed [4], including time reversal techniques [5], the introduction of a scattering source [6–8], or receiver [9] into the brain, computed tomography (CT)-based [10, 11] or MR-based [12] model correction, ultrasound based-correction [13], and magnetic resonance acoustic radiation [14, 15]. In the first steps toward identifying a potentially simpler and more direct means for transcranial ultrasound windowing, we have conducted a study comparing acoustic transmission parameters to those of diffuse infrared transmitted through the skull. The study was originally inspired by the observation that skulls possess certain locations which are relatively

transparent to ultrasound waves. This includes not only the temporal bone window [16], but also locations that can appear on the thicker frontal, occipital, and parietal bones. Unfortunately, the precise locations of such windows tend to vary greatly between different skulls [17]. Casual examination of *ex vivo* skull specimens, however, led us to hypothesize that transmitted light intensity at a given location correlates positively with ultrasound transmission [18], motivating us to explore trends between transmitted optical data and ultrasound data.

The study was performed using infrared light (IL) transmitted through *ex vivo* human skull specimens under the auspice that, should correlation be found between acoustic and optic data, it might motivate further work aimed at detecting similar correlations in a reflection mode and through the scalp. Ultrasound measurements were acquired along the surfaces of skull specimens situated between a transducer and a hydrophone, with the skull surfaces positioned

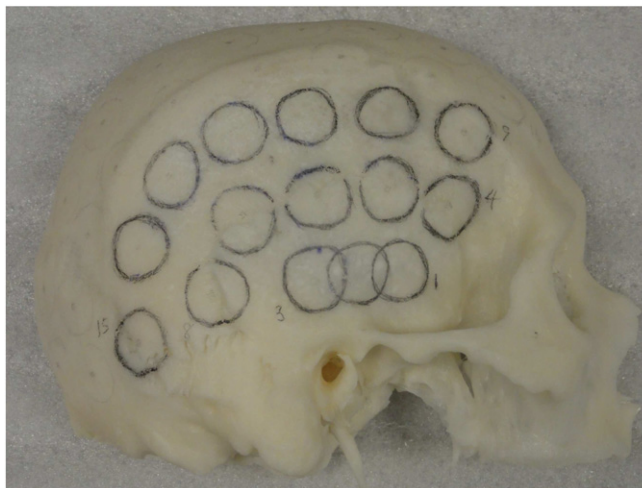


Figure 1. Marked sagittally sectioned half skull. Each marked circle position was numbered as 1, 2, 3, ...

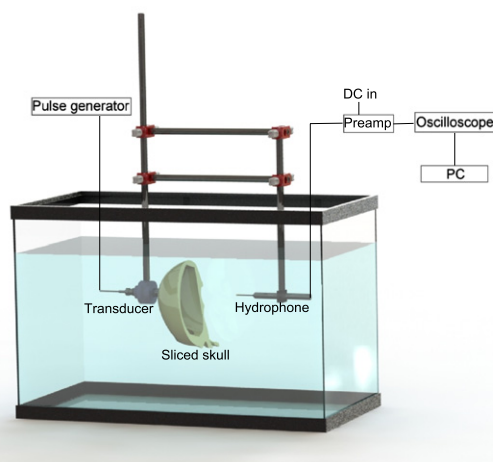


Figure 2. Schematic for ultrasound measurement.

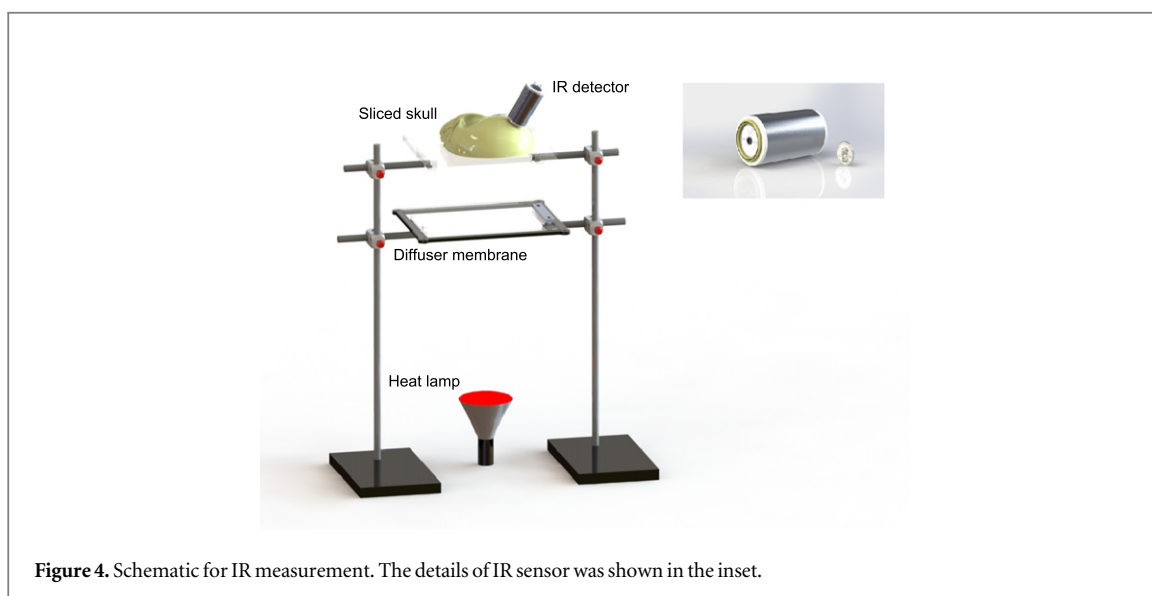
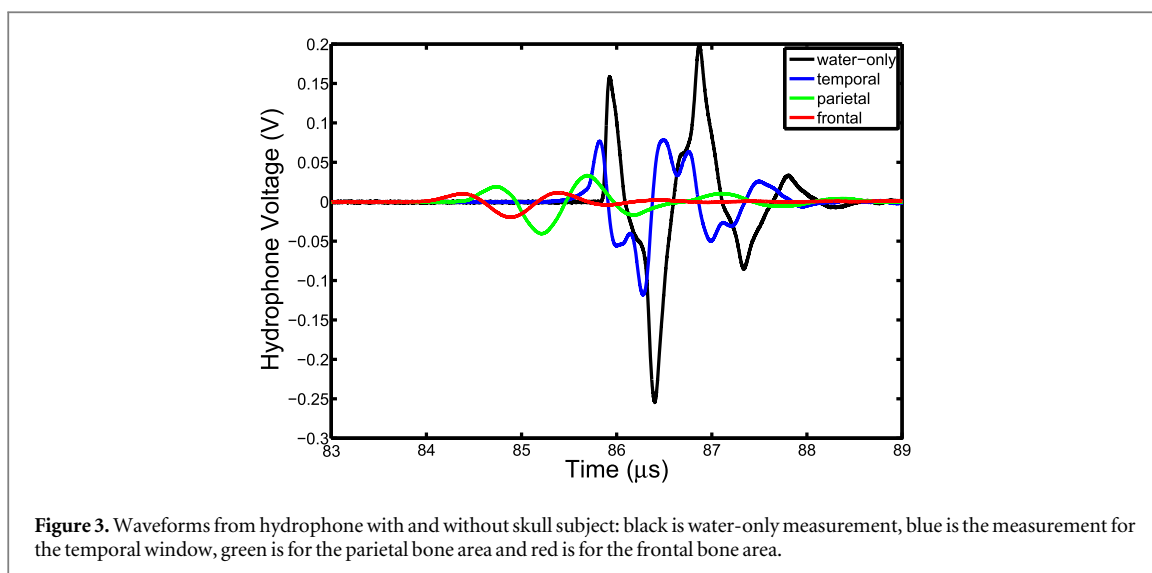
normal to the transducer. Optical measurements were subsequently obtained in a dark room by transmitting IL through the skull sections using an infrared sensor to measure intensity variance on the skull surface.

As shown below, when acoustic amplitudes were compared to the optical intensity, a poor correlation was found. However, a good correlation was observed between the ultrasound time-of-flight (TOF) and optical intensity. The procedure and results of this preliminary work are described below, along with discussion on plausible physical explanation of our findings, and the limitations of this transmission-based study.

2. Methodology

Ultrasound and infrared transmission measurements were performed on nine formalin-fixed skull samples

representing two sagittally sectioned half skulls and seven calvaria, among which two calvaria had intact dura mater. Because the skull is a porous material, one concern was the presence of trapped gases within the *ex vivo* skull bone might affect both the ultrasound and infrared measurement. Therefore one skull specimen was examined before and after degassing. The skull was kept under vacuum for approximately 18 h before repeating the infrared measurement. This skull was then immersed in degassed water and the whole system was degassed for another 20 min before repeating the ultrasound measurement. Excellent before- and after-degassing agreement was found at all measurement locations for both the acoustic and infrared data (the absolute value error for each point is less than 0.6%); so we assumed that only negligible amount of gas was trapped in our formalin-fixed skull specimens, and the degassing process is not essential.



2.1. Ultrasound measurement

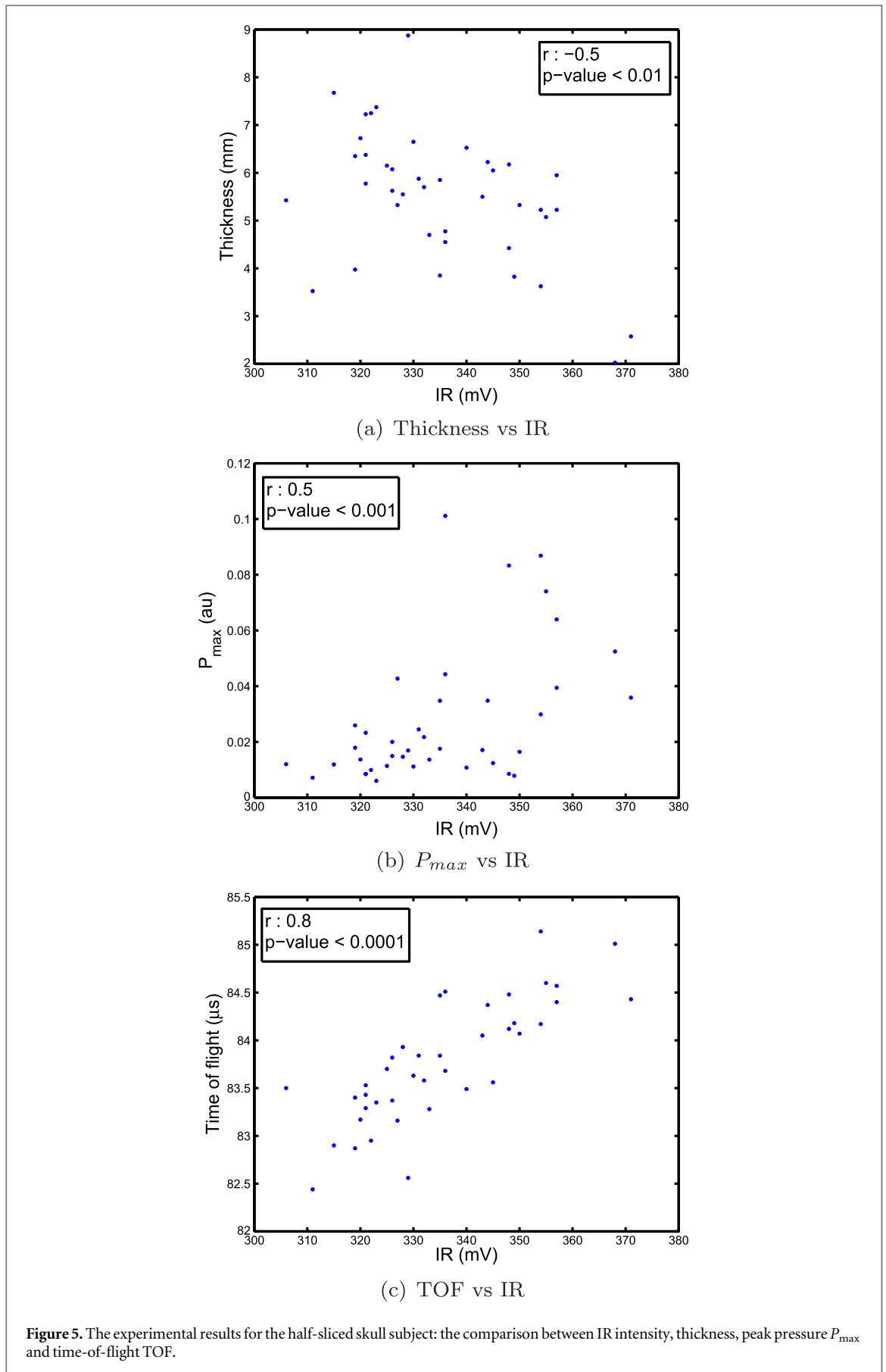
Acoustic signals were transmitted in a water tank between a transducer (Olympus NDT, V303-SU, 1 MHz, 12.7 mm OD, Waltham, MA) and a hydrophone (Onda, HNC-1000, 1 mm diameter active area, Sunnyvale, CA) with and without a skull placed in front of the source transducer. Measurement positions on each skull were physically marked with circles corresponding to the approximate transducer diameter shown in figure 1. For the seven skulls void of dura mater, calipers were used to determine the skull thickness. Four positions in each circle were measured, one at center and three adjacent randomly picked. The ultrasound setup illustrated in figure 2 shows the relative transducer and hydrophone alignment with a separation of approximately 13 cm.

For each measurement location, skulls were placed against the transducer and positioned so that the

transducer was centered about a reference circle and angled approximately parallel to the transducer face. An impulsive voltage was supplied to the transducer (Panametrics 500PR, Waltham, MA), and the resulting hydrophone response was read by an oscilloscope (Tektronix, DPO3034, Beaverton, OR) triggered from the voltage source. The measurement procedure was repeated three times for each position and each time the skull sample was repositioned. No significant changes were found between the three measurements. Four sample waveforms are shown in figure 3: one is water-only measurement, one from the temporal bone window, one from parietal bone and one from frontal bone.

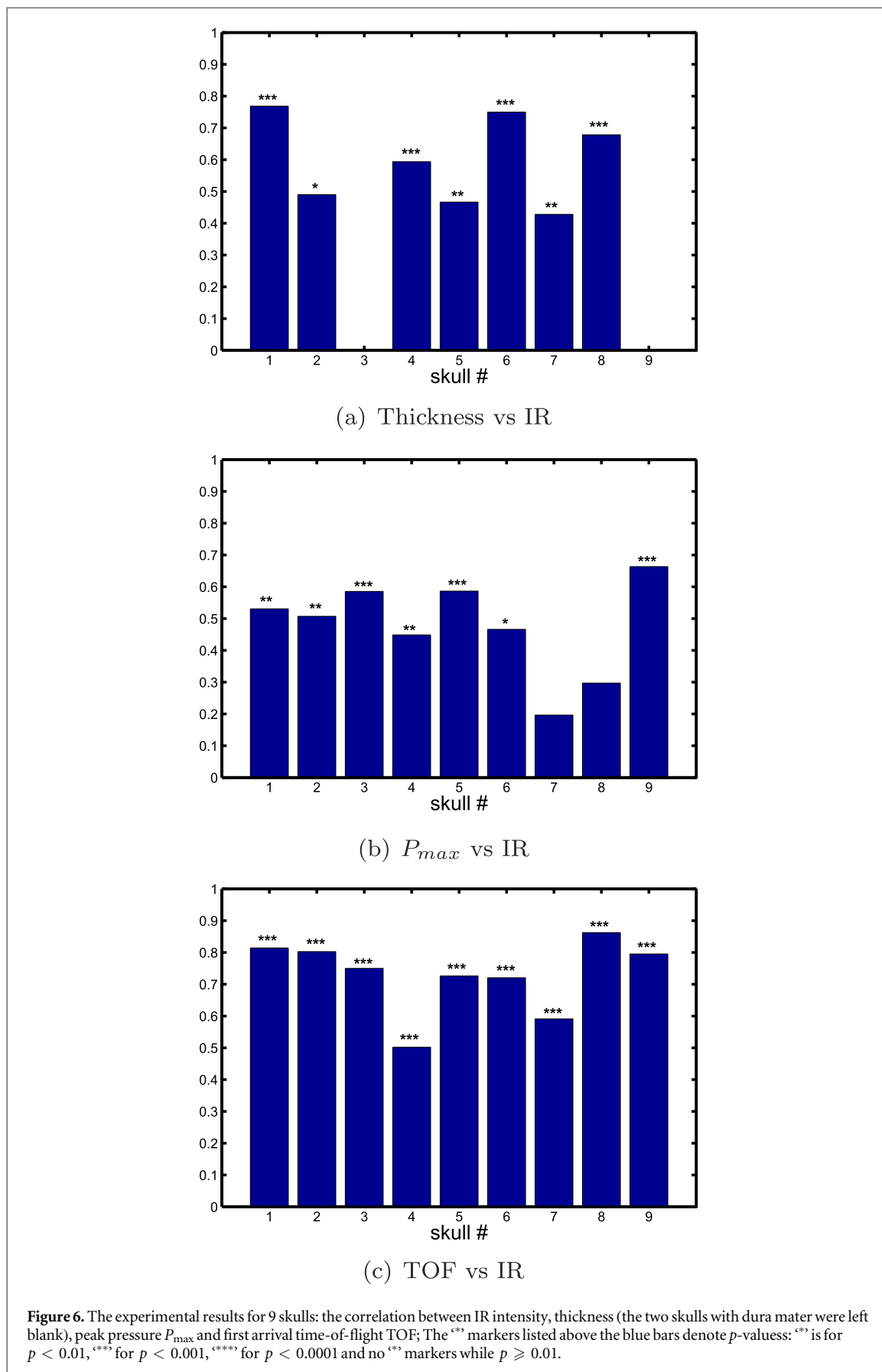
2.2. IR measurement

The optical measurement setup is shown in figure 4. All measurements were performed in a dark room. A



heat lamp (Sylvania, 100 W) was used as a light source and a light shaping diffuser membrane was inserted to obtain uniformly diffused light upon the inner skull

surface. Under this configuration it was assumed that the distribution of infrared intensity over skull location was even. A skull was situated above the



membrane. One infrared sensor (TSAL4400-3 mm, 940 nm), shown in the inset, was embedded in a cylindrical aluminum tube to take infrared

measurement. On the sensor surface, a flexible padding shown as a yellow circle was used for better matching the irregular curved skull surface.

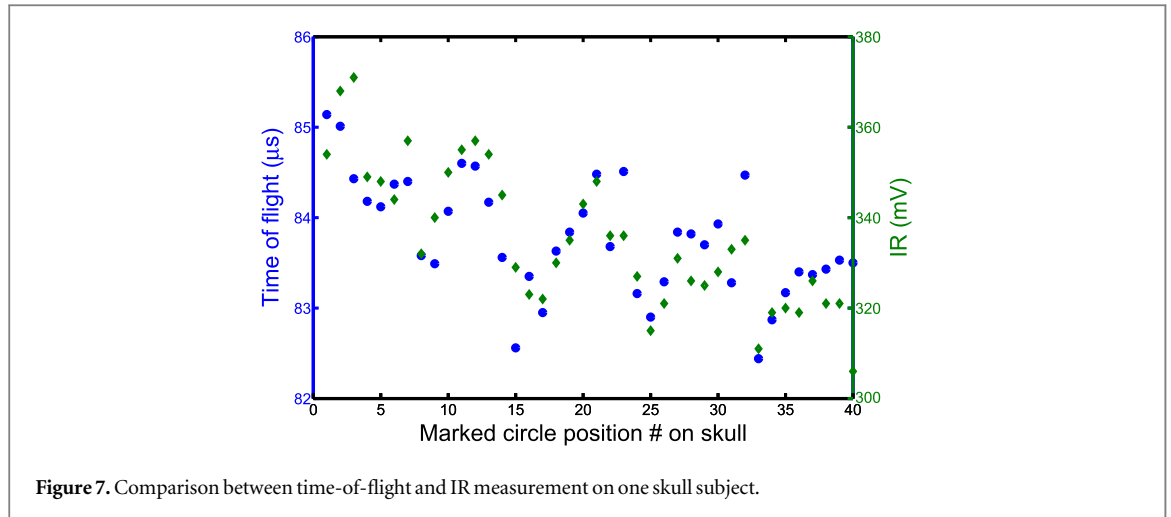


Figure 7. Comparison between time-of-flight and IR measurement on one skull subject.

3. Results

The number of measurement positions attainable by both the ultrasound and optic setups varied, depending on skull size and shape, ranging from 36 to 66 positions (mean = 46) over the nine skulls examined and totaling 417 over all skulls. Data were analyzed to compare relative transmitted optic intensity, skull thickness (L_s), transmitted peak acoustic pressure amplitude (P_{max}) and TOF, defined here as the first detectable time point from the ultrasound signal. Results from one skull sample are shown in figure 5. Both the correlation coefficient and p -values for the data, calculated in Matlab (Mathworks, R2011a, Natick, MA) using the command *corrcoef*, are listed in the inset of each figure.

The correlation coefficients for all skull measurements are shown in figure 6 and the ‘*’ markers on each bar denote the significance of correlation measured by their p -values. Among the nine samples, all p -values between thickness and infrared intensity are below 0.01, which indicates that they correlate. In figure 6(b), it can be seen that skull 7 and skull 8 have poor correlations between peak relative pressure P_{max} (taken directly from the hydrophone voltage) and infrared intensity as the p -value is higher than 0.01. A better and more uniform correlation was found between the TOF and infrared intensity with all p -values less than 0.0001. Figure 7 illustrates TOF and IR intensity as a function of position along one skull surface. It can be seen that the two groups of data correlate well across the entire skull.

Finally, linear regression analysis was performed to study the correlation between infrared intensity and skull thickness, peak acoustic amplitude and TOF for all the nine skulls’ experimental data. Both the linear fit and prediction intervals are calculated and shown in figure 8. The fitted equation for IR and skull thickness L_s is:

$$L_s \{ \text{mm} \} = - 0.11 \{ \text{mm mV}^{-1} \} * IR \{ \text{mV} \} + 40.97 \{ \text{mm} \} \pm 3.5 \{ \text{mm} \} \quad (1)$$

with coefficient of determination $R^2 = 0.53$.

The average human skull thickness is approximately 6.85 mm. An interval of ± 3.5 mm would introduce more than 50% error, which implies that infrared intensity is probably not a good indicator for the thickness estimation.

The fitted equation for IR and peak acoustic pressure P_{max} is:

$$P_{max} \{ \text{au} \} = 0.0006 \{ \text{au mV}^{-1} \} * IR \{ \text{mV} \} - 0.15 \{ \text{au} \} \pm 0.034 \{ \text{au} \} \quad (2)$$

with coefficient of determination $R^2 = 0.24$.

A low R^2 value of 0.24 suggests a weak linear relationship between acoustic energy and optical energy. It is likely because the peak pressure is instantaneous while the infrared intensity measurement is spatially and temporally averaged. This result also explains why some skulls, e.g. skull 7 and skull 8 in figure 6(b), have poor correlation due to different bone structure.

The fitted equation for IR and TOF is:

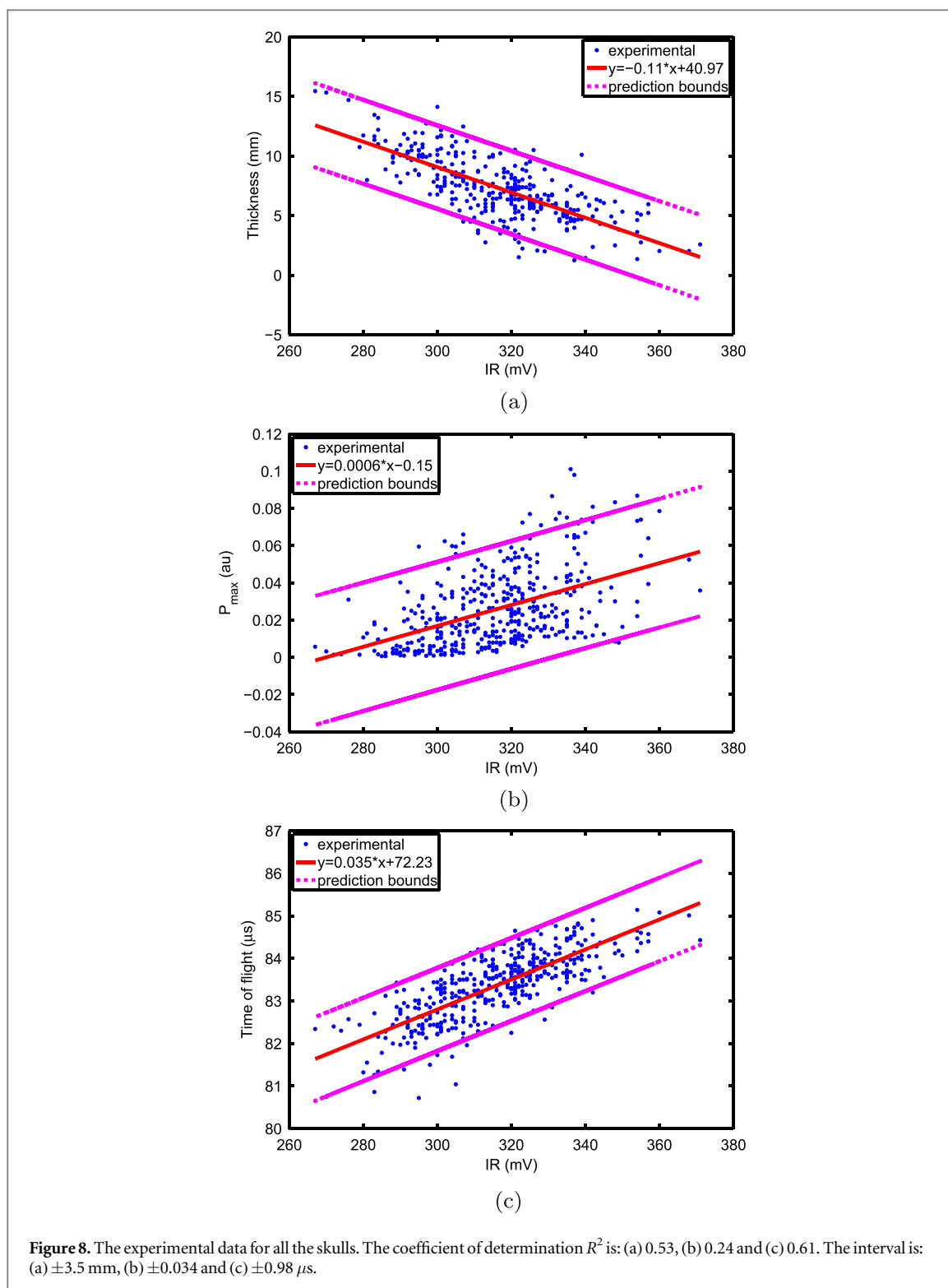
$$TOF \{ \mu\text{s} \} = 0.035 \{ \mu\text{s mV}^{-1} \} * IR \{ \text{mV} \} + 72.23 \{ \mu\text{s} \} \pm 0.98 \{ \mu\text{s} \} \quad (3)$$

with coefficient of determination $R^2 = 0.61$.

For transcranial ultrasound at 500 kHz (which would be used in our transcranial imaging), an interval of $\pm 0.98 \mu\text{s}$ means the degree of error of TOF estimation based on infrared measurement will translate to $\pm 1/2$ of a cycle, which is good enough to focus the beam with a phased array. However, for 1 MHz and above, this interval translates to ± 1 or more cycles, which makes the estimation invalid for guiding the sound beam.

4. Conclusions and discussion

A study with nine *ex vivo* human skulls was performed to examine the correlation between the optic intensity



of diffuse infrared transmitted through the skull and ultrasound transmission. Based on the linear regression analysis of all the nine skull samples, we can conclude that the TOF estimation from the infrared measurement can be potentially used for our transcranial ultrasound focusing.

From figure 8, it can be seen that the infrared intensity inversely correlates to the bone thickness and positively correlates to the acoustic first arrival TOF. Though the full nature of the optical

scattering has yet to be fully investigated, a plausible explanation for correlation between light intensity and TOF entails the skull's layered composition of relatively opaque (acoustically) trabecular bone sandwiched between layers of more transmissive cortical bone (figure 9). Moreover thicker bone tends to correspond to thicker trabecular layers, thus introducing a negative correlation between IR measurements and thickness as well as TOF versus thickness.

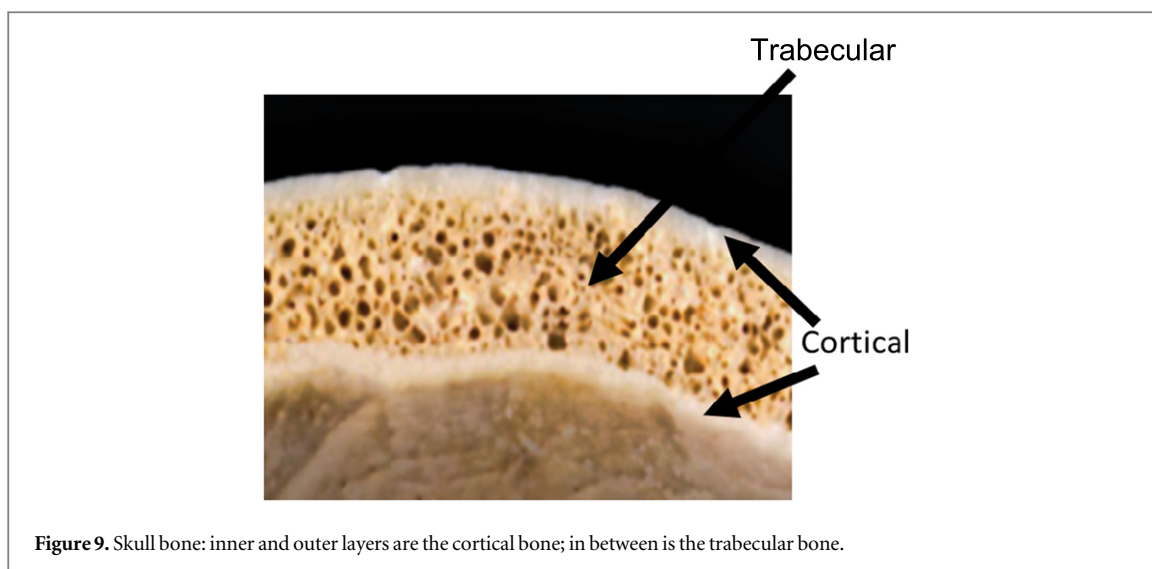


Figure 9. Skull bone: inner and outer layers are the cortical bone; in between is the trabecular bone.

While this correlation study pertains to IR transmission mode, the relationship motivates further study as to whether a similar correlation can be found between backscattered IR and transmission ultrasound. If so, this could have direct application in transcranial ultrasound phase aberration correction [19] given that the light of wavelengths between 650 and 900 nm can penetrate skin and tissues by increasing the incident intensity of light [20].

Acknowledgments

Research reported in this publication was supported in part by the National Institute of Biomedical Imaging and Bioengineering of the National Institutes of Health under award number R01EB014296. The content is solely the responsibility of the authors.

References

- [1] Dussik K T, Dussik F and Wyt L 1947 Auf dem wege zur hyperphonographie des gehirnes *Wien Med Wochenschr* **97** 425–9
- [2] Ballantine H T, Bolt R H, Hueter T F and Ludwig G D 1950 On the detection of intracranial pathology by ultrasound *Science* **112** 525–8
- [3] Smith S W, Trahey G E and von Ramm O T 1986 Phased array ultrasound imaging through planar tissue layers *Ultrasound Med. Biol.* **12** 229–43
- [4] Kyriakou A, Neufeld E, Werner B, Paulides M M, Szekely G and Kuster N 2014 A review of numerical and experimental compensation techniques for skull-induced phase aberrations in transcranial focused ultrasound *Int. J. Hyperth.* **30** 36
- [5] Vignon F, Aubry J F, Tanter M, Margoum A and Fink M 2006 Adaptive focusing for transcranial ultrasound imaging using dual arrays *J. Acoust. Soc. Am.* **120** 2737–45
- [6] Pernot M, Montaldo G, Tanter M and Fink M 2006 Ultrasonic stars for time-reversal focusing using induced cavitation bubbles *Appl. Phys. Lett.* **88** 034102
- [7] Haworth K J, Fowlkes J B, Carson P L and Kripfgans O D 2008 Towards aberration correction of transcranial ultrasound using acoustic droplet vaporization *Ultrasound Med. Biol.* **34** 435
- [8] Gâteau J, Marsac L, Pernot M, Aubry J-F, Tanter M and Fink M 2010 Transcranial ultrasonic therapy based on time reversal of acoustically induced cavitation bubble signature *IEEE Trans. Biomed. Eng.* **57** 134
- [9] Clement G T and Hynynen K 2002 Micro-receiver guided transcranial beam steering *IEEE Trans. Ultrason. Ferroelectr. Freq. Control* **49** 447
- [10] Clement G T and Hynynen K 2002 A non-invasive method for focusing ultrasound through the human skull *Phys. Med. Biol.* **47** 1219–36
- [11] Aubry J F, Tanter M, Pernot M, Thomas J L and Fink M 2003 Experimental demonstration of noninvasive transskull adaptive focusing based on prior computed tomography scans *J. Acoust. Soc. Am.* **113** 84
- [12] Hynynen K and Sun J 1999 Trans-skull ultrasound therapy: the feasibility of using image-derived skull thickness information to correct the phase distortion *IEEE Trans. Ultrason. Ferroelectr. Freq. Control* **46** 752
- [13] Shapoori K, Malyarenko E, Maev R G, Sadler J, Maeva E and Severin F 2009 2D noninvasive acoustical image reconstruction of a static object through a simulated human skull bone *IEEE Int. Ultrasonics Symp. (IUS)* pp 2279–83
- [14] Hertzberg Y, Volovick A, Zur Y, Medan Y, Vitek S and Navon G 2010 Ultrasound focusing using magnetic resonance acoustic radiation force imaging: application to ultrasound transcranial therapy *Med. Phys.* **37** 2934
- [15] Marsac L, Chauvet D, Larrat B, Pernot M, Robert B, Fink M, Boch A L, Aubry J F and Tanter M 2012 MR-guided adaptive focusing of therapeutic ultrasound beams in the human head *Med. Phys.* **39** 1141
- [16] Postert T, Federlein J, Przuntek H and Büttner T 1997 Insufficient and absent acoustic temporal bone window: potential and limitations of transcranial contrast-enhanced color-coded sonography and contrast-enhanced power-based sonography *Ultrasound Med. Biol.* **23** 857–62
- [17] White J, Clement G T and Hynynen K 2005 Transcranial ultrasound focus reconstruction with phase and amplitude correction *IEEE Trans. Ultrason. Ferroelectr. Freq. Control* **52** 1518–22
- [18] Meral F C, Naing Z Z C, Meyer F A, Jafferji M A, Power C, Clement G T and White P J 2014 Transcranial ultrasound-optical transmission correlation *J. Acoust. Soc. Am.* **135** 2209–2209
- [19] Clement G T, White J and Hynynen K 2000 Investigation of a large-area phased array for focused ultrasound surgery through the skull *Phys. Med. Biol.* **45** 1071–83
- [20] Smith K C 1991 The photobiological basis of low level laser radiation therapy *Laser Ther.* **3** 19–24